

Numerical Modeling of Induction Brazing

V. Bruyere¹, C. Durand², S. Roure², P. Namy¹

1. SIMTEC, 5 rue Felix Poulat, Grenoble, France.

2. SCHNEIDER ELECTRIC, Eybens, France.

Abstract

Induction brazing is a widely used joining process in various industries, offering efficient and localized heating for the assembly of diverse components. At Schneider Electric®, this process is used to assemble a silver piece on a copper piece. This work focuses on the advancements and insights gained through the development of a 3D thermal and electromagnetic model with Comsol Multiphysics®. A surface impedance method was used to describe the electromagnetic field in the metal parts. To control the electric power, a global ODE has been added to the problem. Moreover, a strong coupling between electromagnetics and thermal equations has been considered because of the strong variations of electrical conductivity with temperature. Finally, parametric studies have been performed to study the influence of the power cycle and the position of the assembled pieces.

Keywords: Induction Heating, Electromagnetism, Thermal Exchanges, Brazing

Introduction

Induction brazing is a highly efficient and versatile process that enables the joining of different materials through the application of induction heating. This technique utilizes a filler metal (brazing) with a lower melting point than the base materials, allowing a strong and reliable bond between the components. The characteristics of induction heating, such as rapid and localized heating, make it an ideal choice for various applications.

At Schneider Electric®, induction heating can be used to produce electrical contacts consisting of a contact tip, usually a silver-based material, brazed on a copper substrate. The brazing joint between the contact tip and the substrate is formed by the melting of a filler metal positioned in between during the heating of the assembly through an inductor coil properly designed. Induction brazing is commonly used for big contact parts, when resistance welding cannot generate sufficient heat for these dimensions, typically for brazing surface larger than 200 mm². Induction heating is a well understood process, and the use of numerical model is common in the literature [1] [2]. Nevertheless, for complex 3D geometries, specific numerical techniques and correct assumptions must be used to minimize the computational time [3]. The Comsol Multiphysics® software offers a dedicated interface for dealing with this kind of problem and proposes suitable boundary conditions such as surface impedances. Moreover, additional equation can be easily set to customize and enhance the model.

Process Description

The induction brazing process involves joining two dissimilar parts together by means of a filler metal. Figure 1 shows the experimental set-up (top) during

heating. Electric current flows alternately through the inductor, inducing currents in the parts to be heated. Color variations are observable in visible light spectrum (top, Figure 1), highlighting the high temperatures in the part. The part to be assembled is located at the top of the main metal part and is held by four alumina supports all along the process. It is composed of two silver tips marked with blue arrows (top and bottom, Figure 1). The filler metal is placed between the tips to be brazed and the main copper part. A thermal result, presented in more details later in this work, is provided in Figure 1 (bottom), highlighting the 3D geometry used for the model. The inductor and main part geometries are imported with the CAD import module of Comsol Multiphysics®. The alumina supports and the metal tip to be soldered are redesigned manually with the internal geometry builder. The position of the inductor in relation to the parts is parameterized so that its influence can be studied.

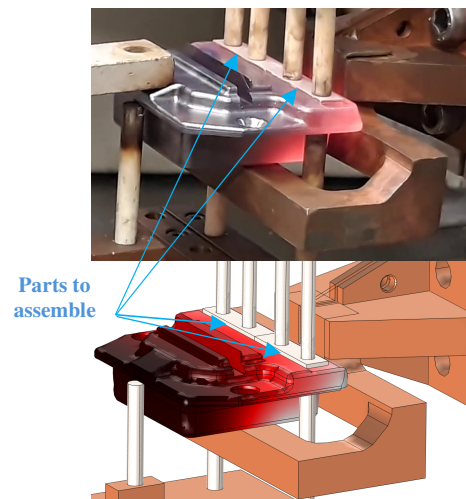


Figure 1. Experimental Set-up (up) and numerical digital twin (down)

Modeling and Governing Equations

Each “physics” solved in Comsol Multiphysics® is detailed with the different assumptions used in this work.

Electromagnetism

The magnetic and electric fields interface is used to compute electromagnetic fields by solving the following Maxwell’s equations:

$$\nabla \cdot \mathbf{J} = 0 \quad Eq. 1$$

$$\frac{1}{\mu_0 \mu_R} \nabla \times \mathbf{B} = \mathbf{J} \quad Eq. 2$$

$$\mathbf{B} = \nabla \times \mathbf{A} \quad Eq. 3$$

$$\mathbf{E} = -\nabla V - j\omega \mathbf{A} \quad Eq. 4$$

$$\mathbf{J} = \sigma \mathbf{E} + j\omega \varepsilon_0 \varepsilon_R \mathbf{E} \quad Eq. 5$$

where \mathbf{J} is the current density vector, \mathbf{B} the magnetic flux density vector, \mathbf{E} the electric field vector, \mathbf{A} the magnetic vector potential, μ the magnetic permeability, ε the electric permittivity and σ the electrical conductivity of the medium.

Given the high frequency used in the process for surface heating the solder, a surface impedance assumption is used. This means that the electromagnetic field is not solved in the volume of the parts to be heated, but only in the surrounding air. As the skin thickness is around twenty times less than the average thickness of the parts, this assumption can be used in this work.

The following boundary condition is applied at the surface of the pieces:

$$\sqrt{\frac{1}{\mu_0 \mu_R \left(\varepsilon_0 \varepsilon_R - \frac{j\sigma}{\omega} \right)}} \mathbf{n} \times \mathbf{B} + \mathbf{E} - (\mathbf{n} \cdot \mathbf{E}) \mathbf{n} = (\mathbf{n} \cdot \mathbf{E}_s) \mathbf{n} - \mathbf{E}_s \quad Eq. 6$$

with \mathbf{E}_s the source electric field.

The potential $V = V_0$ is applied at the inlet of the inductor and the potential $V = 0$ is applied at the outlet. In order to obtain a precise value of the resulting intensity, Lagrange multipliers (“weak constraints”) are used. It is indeed required to precisely control the electromagnetic power.

Power Control

As the electrical power is measured at the generator and the electrical circuit is not simulated in this initial study, a numerical power supply seems to be the most accurate method to supply the inductor. An extra-ODE is used to apply the power to the inductor at each time step by solving the following equation:

$$\iint \frac{1}{2} Re\{V_0 I^*\} dS_{ext} - P_{ref}(t) = 0 \quad Eq. 7$$

with V_0 the variable electric potential and I^* , the conjugate of the resulting current intensity through the external surface S_{ext} and $P_{ref}(t)$ the applied power set as a function of time.

The initial value of the electric potential V_0 must be carefully close to the final value to avoid numerical issues.

Moreover, as the electrical conductivity of the material to be heated is a strong function of temperature, a coupled resolution with heat equation is necessary. As the inductor is sufficiently well cooled, the influence of temperature rise in the inductor is considered negligible on variations in electrical conductivity.

Thermal Exchanges

Due to the high current flowing through the metal pieces, thermal energy is generated. The following energy equation is solved in the metal pieces:

$$\rho C_p \frac{\partial T}{\partial t} + \nabla \cdot [-k \nabla T] = 0 \quad Eq. 8$$

where T is the temperature, ρ the density, k the thermal conductivity and C_p the heat capacity of the material.

Due to skin effect, Joule effect is considered as a boundary condition by setting the heat flux:

$$-\mathbf{n} \cdot (-k \nabla T) = \frac{1}{2} Re\{\mathbf{J} \cdot \mathbf{E}^*\} \quad Eq. 9$$

Natural convection and ambient radiation are also taken into account on the exterior boundaries by:

$$-\mathbf{n} \cdot (-k \nabla T) = \varepsilon \sigma (T_{amb}^4 - T^4) + h(T_{amb} - T) \quad Eq. 10$$

with ε the emissivity of the surface, σ the Boltzman constant, h a heat coefficient T_{amb} the ambient temperature.

The latent heat of the brazing has been neglected given its small volume.

Model Validation

Numerical Aspects

As the electrical conductivity of the simulated materials varies greatly with temperature, it is necessary to solve the electromagnetic problem at each time step of the thermal problem. A “frequency-transient” step is thus used. Due to the power control ODE, time step must be carefully constrained by specifying a maximum value for the BDF solver. A segregated non-linear solver is used to reduce the computational time.

To validate the spatial and temporal discretization used for the resolution of this coupled problem, a

power balance is performed. The normalized power evolutions are plotted in Figure 2 as a function of time divided by the reference duration τ .

The electric power is computed (in blue, Figure 2) by integrating the heat flux due to Joule effect on the exterior surfaces S_{ext} :

$$\iint \frac{1}{2} Re\{\mathbf{J} \cdot \mathbf{E}^*\} dS_{ext} \quad Eq. 11$$

The resulting variation of enthalpy (in green, Figure 2) in the thermal domain $V_{thermal}$ is defined by:

$$\iiint \rho C_p \frac{\partial T}{\partial t} dV_{thermal} \quad Eq. 12$$

Finally, the losses by radiation (Eq. 13 and in red, Figure 2) and by natural convection (Eq. 14 and in cyan, Figure 2) are evaluated on the exterior surfaces S_{ext} :

$$\iint \varepsilon \sigma (T_{amb}^4 - T^4) dS_{ext} \quad Eq. 13$$

$$\iint h(T_{amb} - T) dS_{ext} \quad Eq. 14$$

The sum of the enthalpy variation and all the losses (plotted with magenta markers in Figure 2) should be equal to the heat source (electrical power). This has been verified for an accuracy of less than 1%.

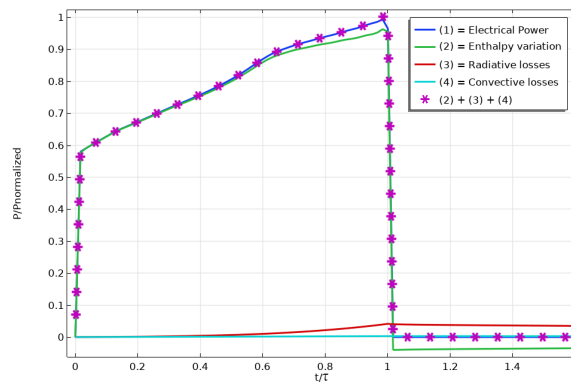


Figure 2. Power balance in the heated parts

It can be noticed that radiative losses become non negligible at the end of the heating phase close to $t = \frac{3\tau}{4}$ due to high temperatures reached at the end of the process. The convective losses remain negligible throughout the entire process.

Experimental Validation

To validate the model, a qualitative comparison with experimental results is performed. Since the temperature range in which the solder reaches its melting point is known, the reference configuration (nominal configuration) is studied. This corresponds to a power cycle and an inductor position allowing the solder to melt completely and correctly. The numerical results are shown in Figure 3 at the end of

the heating phase. For confidentiality reasons, the numerical results are scaled down throughout this work. The green zone represents the region for which the temperature is at the solder melting temperature with a confidence interval of $\pm 5\%$. The red zone represents temperatures that are too high, and the blue zone represents temperatures that are too cold. If the temperature is too low, the solder will not melt completely or at all, leading to poor assembly. If the temperature is too high, the brazing filler can be modified, reducing the quality of the product. Controlling the brazing temperature is therefore crucial for the quality of the assembly.

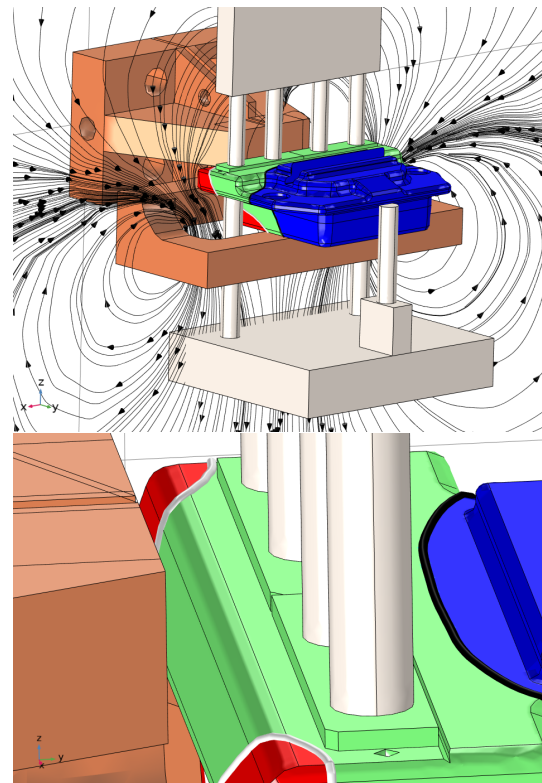


Figure 3. Temperature zones in the heated parts for nominal operating conditions (Top: global view, Bottom: local view) – Black and white contours delimit the acceptable temperature zone in green – Black streamlines and arrows represent the magnetic flux density

As can be seen in Figure 3, the tips to be assembled are within the confidence interval (in the green region) for this nominal configuration, thus validating the numerical model developed. It can also be used to study the local temperature gradients and their role on the assembly quality. The temperature (normalized by the melting temperature of the brazing) is plotted in Figure 4 at the brazing interface between the tip and the main metal part, at the end of the heating process. All the points have exceeded the melting temperature. The hottest areas can be identified, and they correspond to areas where modified brazing alloy plus braze flow problems have been identified experimentally under more intense brazing conditions.

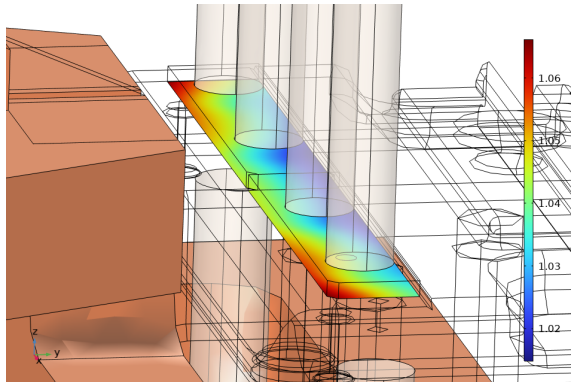


Figure 4. Temperature at the brazing interface normalized by the melting temperature at nominal operating conditions

Thanks to these numerical and experimental validations, the model can now be used to simulate the influence of the inductor position and the power temporal profile.

Benefits of the digital twin

The major advantage of this simulation lies in its flexibility for studying the influence of different parameters. In future work, it will also be possible to study the influence of inductor geometry to further optimize the process. We will focus here on the influence of the position of the inductor and on the power time profile.

Influence of the inductor position

The inductor position is a very critical aspect. Indeed, it governs the power transmitted to the metal part (efficiency) and must be precisely adjusted. To study quantitatively its influence, the inductor is approached in the y-direction to the part by a value of Δ (at the top, Figure 5). The nominal configuration is shown in the middle Figure 5. And at the bottom Figure 5, the inductor is moved away from the part by the same Δ value. The δy parameter represents the deviation from the original position. The resulting minimal temperature in the brazing is plotted for these three configurations in Figure 6. The same electrical power is applied for each configuration.

The sensitivity of the model to this parameter is very important. If the inductor is too close to the parts the temperature becomes too high throughout the brazing area, and if it is too far, the melting temperature is not reached. The same study was carried out in the z-direction to validate the original position and to give a tolerance interval to ensure required assembly quality.

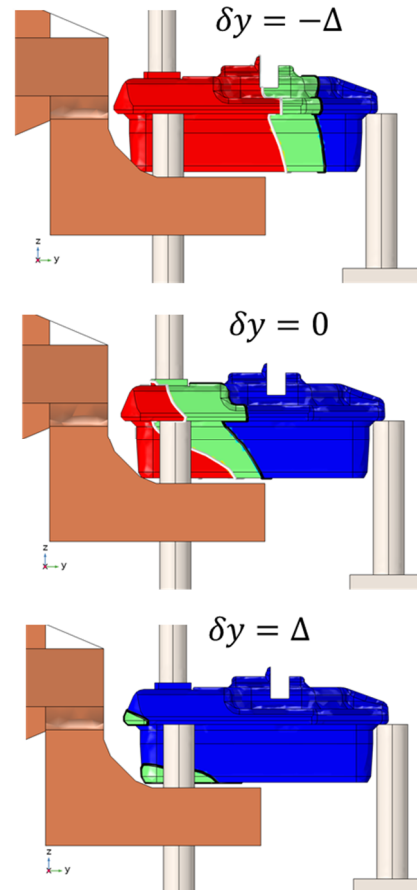


Figure 5. Temperature zones in the heated parts for the three positions of the inductor

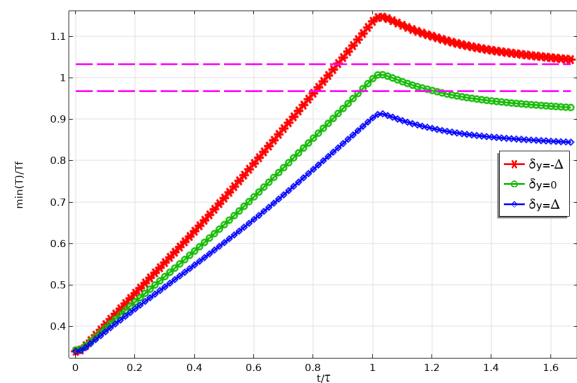


Figure 6. Minimal temperature in the brazing interface normalized by the melting temperature for three inductor positions

Influence of the power cycle

Another important element of the process is the electrical power supply and the related heating time. As discussed previously, the temperature in the brazing must be within a certain range to guarantee a good quality of assembly. However, temperature uniformity is also important as well as the time required to reach this temperature. To improve production line efficiency, heating time is indeed a key factor that needs to be optimized.

To study this aspect, three power profiles are simulated. They are plotted in Figure 7: power is

increased by 20% for the red curve compared with the reference power in green. It is reduced by 20% for the blue curve. The duration of the heating phase is adapted for each configuration to obtain the same minimal temperature in the brazing, plotted in Figure 8.

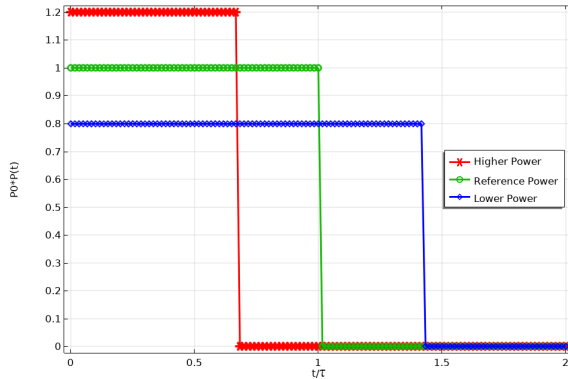


Figure 7. Power profiles for the three study configurations as a function of time

As expected, the time taken to reach the same minimum temperature in the brazing is shorter for the highest power and longer for the lowest power. Temperature heterogeneity is estimated by calculating the following indicator in the brazing: $\frac{\max(T) - \min(T)}{\min(T)}$. It is drawn in Figure 9 for the three study powers. The higher the power, the faster the minimum required temperature is reached, and the greater the heterogeneity. The model can then be used to determine the optimum power profile to achieve minimum heating time while guaranteeing acceptable homogeneity.

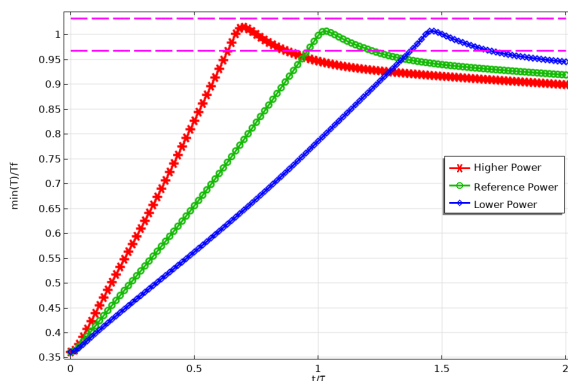


Figure 8. Minimal temperature in the brazing interface normalized by the melting temperature for three different powers

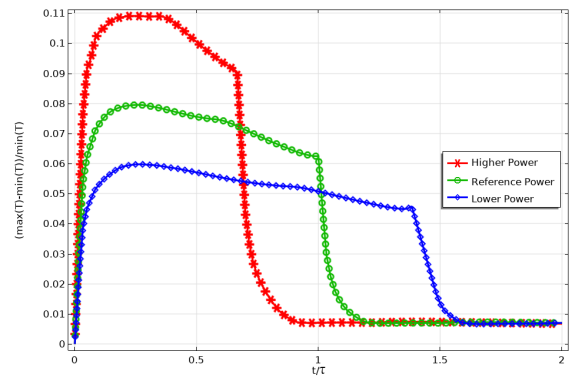


Figure 9. Difference between maximum and minimum temperature in the brazing divided by the minimal temperature for three different powers

A spatial representation of temperature ranges is presented in Figure 10, at the time when the maximum temperature is reached for each configuration. For the highest power (at the top, Figure 10), the brazing temperature is in the red part. For the lowest power (at the bottom, Figure 10), the brazing is in the green zone and the homogeneity is better (in blue, Figure 9). However, the heating time is 40% longer, making it impossible to meet production constraints.

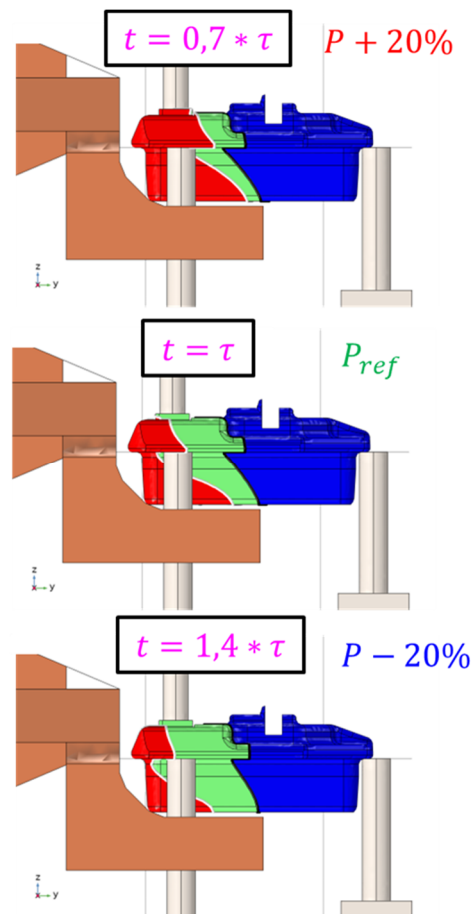


Figure 10. Temperature zones in the heated parts for the three power profiles

Conclusions

An electromagnetic thermal model of induction brazing has been developed in this work. A power control has been adapted to allow precise comparison of thermal results for different configurations. The surface impedance method was used to limit calculation time while maintaining satisfactory accuracy. Numerical validation was proposed to validate the mesh and time step used.

Thanks to this digital twin, parametric studies could be carried out around a reference configuration. These were used to validate the operating conditions (position, power) used for this inductor geometry and parts to braze. The process parameters can now be precisely adjusted using the numerical model. In addition, after validation on this reference configuration, the model can also be used to treat other geometries of parts to be heated. The geometry of the inductor is also a key factor in improving efficiency while controlling the temperature distribution throughout the parts. Finally, thanks to the flexibility of Comsol Multiphysics®, the metallurgical aspects can also be studied in a future project.

References

- [1] P. Bocher, "Simulation of Fast Induction Surface Heating and Comparison with," in *International Conference on Heating by Electromagnetic*, Padua, 2013.
- [2] A. Nikanorov, "Approaches for Numerical Simulation of High Frequency Tube Welding Process," 2013.
- [3] J. Jin, *The finite element method in electromagnetics*, Wiley New York, 2002, pp. 22-23.